Proton Spin Relaxation of a Liquid Crystal with a Glassy Cholesteric State

D. Pusiol* and F. Noack,
Physikalisches Institut der Universität Stuttgart

C. Aguilera**,
Institut für Makromolekulare Chemie der Universität Freiburg

Z. Naturforsch. **45 a**, 1077–1084 (1990); received June 8, 1990

Field-cycling and standard pulsed NMR techniques have been used to study the frequency dependence of the longitudinal proton spin relaxation time T_1 in the crystalline estradiol compound (+)3,1,7-β-bis-(4n-butoxybenzoyloxy)-estra-1,3,5-(10)-trien or *BET*, which is a mesogenic material with a chiral molecular structure. From the measured Larmor frequency and temperature dependences we conclude that, at *low NMR frequencies* in the cholesteric phase, T_1 reflects in addition to the relaxation process familiar from nematic liquid crystals (director fluctuation modes) another slow mechanism theoretically predicted for cholesteric systems, namely diffusion induced rotational molecular reorientation. These relaxation processes are not or much less effective in the crystalline and glassy state, where they are frozen. Also the *high NMR frequency* relaxation dispersion strongly differs between the cholesteric mesophase and the not liquid crystalline samples. This is interpreted by a change from essentially translational self-diffusion to rotational diffusion controlled proton relaxation.

1. Aim of this Work

Molecular motions in cholesteric liquid crystals are more intricate than in untwisted mesogens because of the long-range helical ordering of the average orientation of the molecules. This circumstance complicates most spectroscopic approaches to analyse and separate the various kinds of motional processes, like translational self-diffusion along different axes and individual or collective rotational reorientations of whole molecules or special segments. In the following, we briefly describe a Larmor frequency dependent study of the longitudinal proton relaxation time T_1 for the cholesteric liquid crystalline estradiol compound (+)3,1,7-β-bis-(4n-butoxybenzoyloxy)-estra-1,3,5-(10)-trien, henceforth denoted by *BET*. Up to now, only very few spin relaxation measurements of cholesteric mesophases have been described in the literature [1–4]. In particular, there exist no frequency dependent measurements over a range sufficient to allow a satisfactory separation of the underlying intensity spectra of different molecular reorientation mechanisms.

Available experimental data on the longitudinal proton relaxation of cholesteric liquid crystals essentially show two complications in comparison with results for untwisted nematic systems, namely: On the one hand, the longitudinal magnetization decay is often non-exponential [1], i.e. not fully explicable by a single time constant T_1. On the other hand, it has been pointed out that the self-diffusion of molecules along the helix axis should induce a special rotational relaxation contribution typical for cholesteric systems [4–6] (diffusion induced rotation or *DR*) which, however, has not been observed so far. Remarkably, this kind of reorientation and its time scale are well-known from the related changes of the proton NMR spectrum [7], so that it is surprising indeed not to have seen effects on the relaxation rate.

The main purpose of this report is to demonstrate the presence and importance of the DR relaxation contribution in a *cholesteric* mesogen in addition to the familiar proton relaxation processes dominating in *nematic* liquid crystals [8–10], like e.g. director fluctuation modes, self-diffusion or strongly hindered anisotropic molecular rotations. Its effect on T_1 is clearly demonstrated by measurements of the Larmor frequency dependence, i.e. the dispersion profile $T_1(\nu)$, over the broad range of frequencies $\nu = \omega/2\pi$ accessi-

* Permanent address: Facultad de Matemática, Astronomía y Física, Universidad Nacional de Córdoba, 5000 Córdoba, Argentina.
** Permanent address: Departamento de Química, Facultad de Ciencias, Concepción, Chile.

Reprint requests to Prof. Dr. F. Noack, Physikalisches Institut der Universität Stuttgart, 7000 Stuttgart-80, Pfaffenwaldring 57, BRD.

0932-0784 / 90 / 0900-1077 $ 01.30/0. – Please order a reprint rather than making your own copy.

ble by means of fast NMR field-cycling techniques. We considered the estradiol compound BET [11] to take advantage of the also available glassy state of this cholesteric mesogen, where the cholesteric order can be frozen. Since in this sample the relaxation decay is in good approximation singly exponential, the problem of non-exponentiality will be discussed for some more suitable systems in a separate paper [12].

2. Sample Preparation and Experimental Techniques

Estradiol liquid crystals, including BET, were first synthesized and described by Hoffmann et al. [13, 14]. In the present work, BET was prepared by a different method, which yields a better output [11]. Our synthesis is based on the reaction between estradien-(1,3,5)(10)-diol-(1,1,7,β) and 4-n-butoxy-benzenechloride (weight ratio 1.02:1.59) at 90 °C. This temperature is maintained until the formation of hydrochloric acid HCl ceases. At this stage, the temperature has to be slowly increased to complete the reaction, and after that the HCl is washed out by a nitrogen stream. Finally, the estradiol compound is cooled and recrystallized from ethanol. We found a yield of 89%, compared with 48% reported by Hoffmann et al. The molecular structure of BET was confirmed by a NMR spectrum analysis and is shown in Figure 1. Using a Perkin-Elmer DSC-7 differential scanning calorimeter, it was possible to observe several phases of the compound, which were assigned to a crystalline, glassy, cholesteric liquid crystalline, and isotropic liquid state of the material, respectively. Table 1 lists the transition temperatures and enthalpies between these states for further reference. Note that between heating or cooling the material there exist strong hysteresis effects as illustrated by Fig. 2, which made our relaxation measurements rather lengthy.

The measurements of the longitudinal proton relaxation dispersion $T_1(\nu)$ in the different states of BET were performed by field-cycling and standard pulsed NMR in the Larmor frequency range from about 1 kHz to 70 MHz. Above 10 MHz we used a conventional frequency variable spectrometer [15], whereas the low-frequency data were obtained by means of a home-built field-cycling apparatus [10]. With both instruments the random error of the individual T_1 points is less than 10% after appropriate signal averaging, and the sample temperature can be controlled with an accuracy of at least 0.5 °C. The experimental

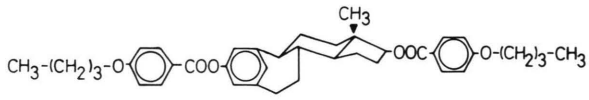

Fig. 1. Molecular structure of (+)1,3,7-β-bis-(4-n-butoxy-benzoyloxy)-estra-1,3,5-(10)-trien (BET).

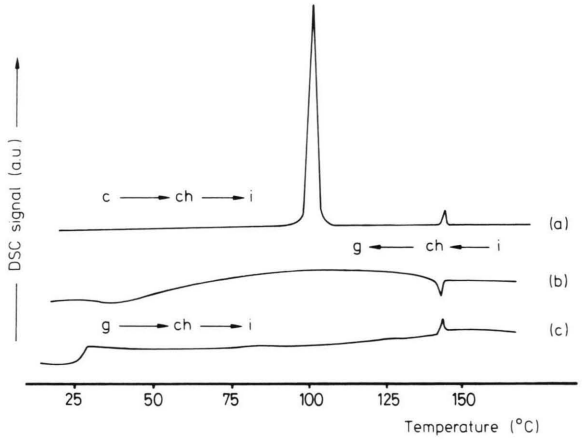

Fig. 2. Differential scanning calorimetry plots of BET for three sample treatments: (a) Heating from the crystalline to the cholesteric and isotropic states; (b) cooling from the isotropic to the cholesteric and glassy states; (c) heating from the glassy to the cholesteric and isotropic states.

Table 1. Phase transition temperatures and transition enthalpies of BET for different sample treatments (c = crystalline; g = glassy; ch = cholesteric; i = isotropic).

Thermal treatment	Transition temperature ϑ/°C	Transition energy Δ/(J g^{-1})
First heating	100 143 c ↦ ch ↦ i	48 0.7 c ↦ ch ↦ i
Cooling	143 37 i ↦ ch ↦ g	0.8 – i ↦ ch ↦ g
Second heating	28 143 g ↦ ch ↦ i	– 0.7 g ↦ ch ↦ i

error of the frequency ν or the underlying magnetic field strength is negligible compared with that of T_1, since the linear current-field relation allows a very exact calibration of the ν scale.

In order to obtain a reproducible T_1 result at a selected temperature ϑ in view of the strong hysteresis of the phase transitions (Table 1), the temperature adjustments had to be preceded by a suitable thermal treatment of the sample. We applied the following procedures: Before starting the T_1 measurements at a

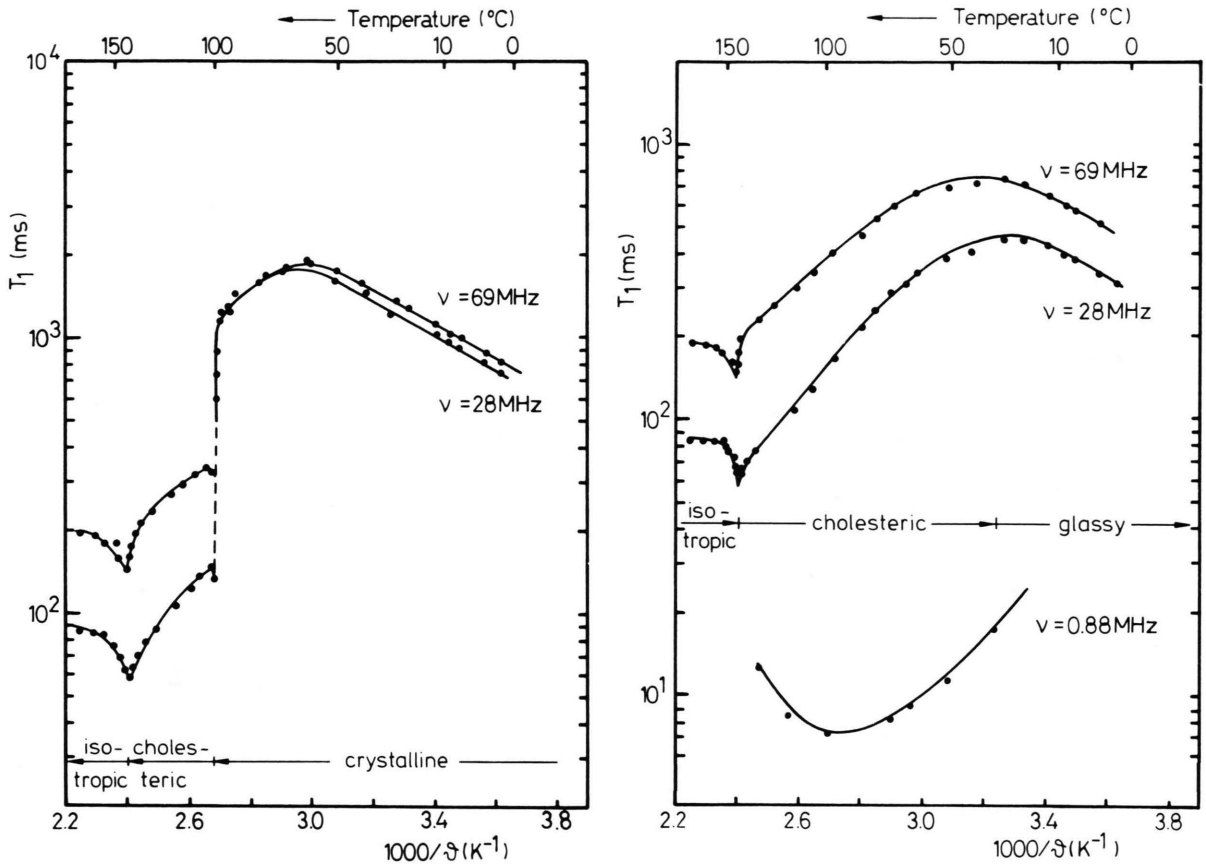

Fig. 3. Temperature dependence of the longitudinal proton relaxation time of BET at several Larmor frequencies for two sample treatments: (a) Heating from the crystalline to the cholesteric and isotropic state; (b) cooling from the isotropic to the cholesteric and glassy state.

temperature in the *cholesteric* or *glassy* phase, the sample was heated to the isotropic state, then cooled to room temperature ($\sim 20\,^{\circ}C$) with the maximum magnetic field (0.25 T) of our field-cycling spectrometer on, and finally heated or cooled to the desired temperature of the T_1 experiment. These steps are related to the calorimeter plots (b) and (c) in Fig. 2, respectively. The T_1 measurements in the *crystalline phase* were performed after recrystallization of the material from ethanol, and then directly adjusting ϑ without crossing the solid-to-cholesteric phase transition, i.e. by a treatment related to plot (a). Instead of this unwieldy chemical recrystallization the crystalline phase could also be produced from the glass by maintaining the sample temperature near 40 °C for about one week without the magnetic field of the spectrometer on, or for about one day when applying the maximum available magnetic flux density. We checked the equivalence of both preparation procedures through the form of the proton NMR signal after a 90°-radio-frequency pulse (free induction decay), and also by the optical behaviour of the sample (transparence of the crystalline phase instead of selective reflection for both the glassy and cholesteric phases). Note from the positions of the exothermic or endothermic DSC peaks shown in Fig. 2 that the cholesteric range is much broader above the glassy than above the crystalline state of the compound.

3. Experimental Results and Discussion

To illustrate the effects of phase transitions and hysteresis on the T_1 proton spin relaxation of BET, and in particular the behaviour in the cholesteric state, Fig. 3 shows our experimental $T_1(\vartheta)$ results by log T_1 versus

$1/\vartheta$ plots at several Larmor frequencies ν (0.88, 28 and 69 MHz) for the two described sample treatments, namely: (i) On heating the sample from the crystal (Fig. 3a), and (ii) on heating it from the glass (Fig. 3b). In the first case it was not possible to make reliable measurements at 0.88 MHz because of the too poor signal-to-noise ratio obtained from the solid compound. Qualitatively, the high-frequency plots are similar in both diagrams, which means that there exists a negative $T_1(1/\vartheta)$ slope at low temperatures, a positive $T_1(1/\vartheta)$ slope at higher temperatures, and discontinuities above $\vartheta \approx 100\,^{\circ}\mathrm{C}$. But obviously the details look very different. In particular, the position of the T_1 maximum is strongly shifted between the crystalline-to-cholesteric and the glassy-to-cholesteric temperature cycles, respectively. Also the Larmor frequency dependence of the T_1 plots is much weaker in the crystalline than in the glassy state of the sample.

Comparison of these data with the positions of the DSC peaks in Fig. 2 reveals that the T_1 maximum in Fig. 3b at $\nu \approx 40\,^{\circ}\mathrm{C}$ reflects the glass-to-cholesteric transition, whereas the corresponding maximum in Fig. 3a at $\vartheta \approx 60\,^{\circ}\mathrm{C}$ cannot be directly related to a DSC peak, and thus has to be ascribed to pretransitional effects of the crystal-to-cholesteric transformation. This structural change is also clearly seen in the range from 40 to 50 °C by the lengthening of the free induction decay from about 15 μs to 80 μs, i.e. by more than a factor of five. The observed high-temperature discontinuities of T_1 develop on the one hand between the crystalline and cholesteric state, and on the other between the cholesteric and isotropic state, but not at the glass-to-cholesteric transition. This demonstrates that the effective relaxation mechanism is similar for the glassy and the liquid crystalline sample. Furthermore, at temperatures above the crystal-to-cholesteric transition, the T_1 results agree with the measurements which begin with the glassy phase, i.e. in this range memory effects due to the sample treatment are, if any, within the experimental error limits. Finally, the additional low-frequency plot in Fig. 3b illustrates that, on a slower time scale, the dominating relaxation process in the cholesteric state runs through a shallow yet clearly visible minimum; such a relaxation behaviour is not known from the numerous relaxation studies of untwisted nematic mesophases [9, 10].

We now concentrate on the results for the cholesteric liquid crystalline sample. To analyse the underlying molecular reorientations via the characteristic frequency dependence of the spectral intensities of the magnetic coupling between proton spins [10, 16], the proton relaxation time T_1 was also studied in its dependence on the Larmor frequency at two selected temperatures, namely at 50 °C (near the glass-to-cholesteric transition). Qualitatively, the dispersion profiles shown in Figs. 4 and 5 are rather similar to results reported in the literature for numerous untwisted nematic compounds [8–10], i.e. they have a low-frequency plateau up to about 10 kHz, followed

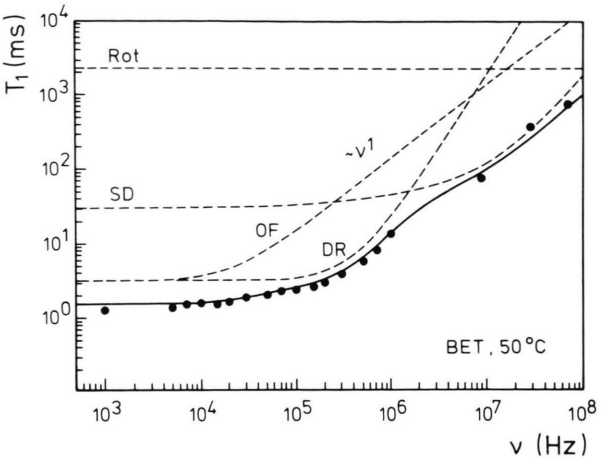

Fig. 4. Larmor frequency dependence of the longitudinal proton relaxation time of BET in the cholesteric phase at 50 °C. The points are experimental data, the full line shows the theoretical curve fit according to (1)–(5), and the dotted lines illustrate the individual relaxation contributions.

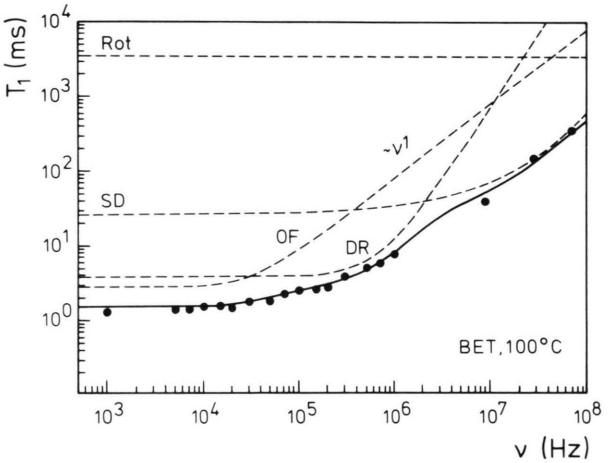

Fig. 5. Larmor frequency dependence of the longitudinal proton relaxation time of BET in the cholesteric phase at 100 °C. The notation is as in Figure 4.

by a strong T_1 increase. This increase, as better seen by the plot at 50 °C than by that at 100 °C, involves a point of inflection for $\nu \approx 5$ MHz and thus separates the time scales of (at least) two different mechanisms. Curve fitting attempts to describe the data by means of the dominating relaxation processes of nematic mesogens, namely nematic order fluctuations [17, 18] (OF) in the kHz range and molecular self-diffusion [19] (SD) in the MHz range, failed as expected, mainly since such a handling does not consider the unusual $T_1(\vartheta)$ minimum of Fig. 3 b in the low-frequency range. This minimum requires that one has to include an additional relaxation contribution at low ν's which allows to descibe the change of the $T_1(1/\vartheta)$ slopes not predicted by the order fluctuation model [17, 18]. We added the diffusion induced rotation process (DR) first suggested by Andreev [5] and later refined by Žumer et al. [6], because it is reasonable to assume that this process is sufficiently slow to influence the low-frequency dispersion. Such curve fits did also not lead to a satisfactory improvement at low Larmor frequencies, where the experimental dispersion profile turned out to be much too steep. The main reason for this inadequacy was found to be the broad square-root law $T_1 \sim \nu^{1/2}$ dependence involved in the OF contribution, which could not be made compatible with the steeper experimental $T_1 \sim \nu^1$ behaviour. Similar effects have been observed previously for other cholesteric mesogens [12], so that at the moment there exist strong evidences that the spectrum of order fluctuations is different in nematic and cholesteric liquid crystals. As a suitable alternative, we applied Blinc et al.'s more recent $T_1 \sim \nu^1$ OF relaxation model [20, 21], originally developed for smectic-type, i.e. two-dimensional order fluctuation modes. In our case this could imply the assumption of a strongly hindered or even absent collective mode propagation perpendicular to a plane with parallel director field, i.e. parallel to the helix axis.

Hence we tried a quantitative interpretation of our $T_1(\nu)$ data in terms of a superposition of three distinctly frequency dependent relaxation contributions, namely: (i) order fluctuations (OF) with a characteristic $T_1 \sim \nu^1$ range, (ii) self-diffusion (SD) with a characteristic $T_1 \sim \nu^{3/2}$ range, and (iii) diffusion induced rotation (DR) with a predicted $T_1 \sim \nu^2$ range. The possibility of a forth, more or less frequency independent term (iv) due to fast rotations of molecular segments or whole molecules [22, 23] (Rot) was included for completeness, though previous studies of untwisted nematic mesophases revealed only minor effects on the T_1 dispersion profiles [8–10, 23].

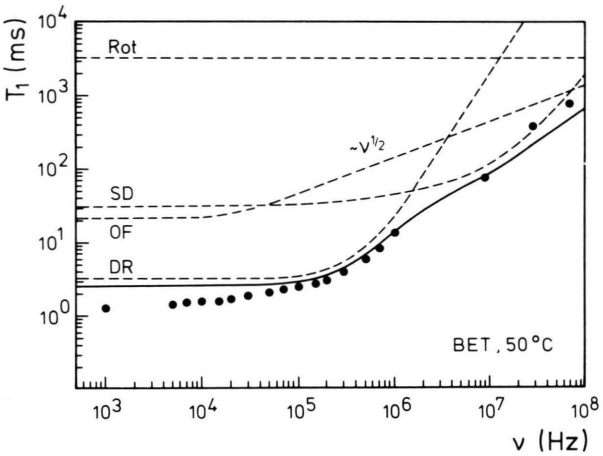

Fig. 6. Experimental $T_1(\nu)$ data of Fig. 4 with unsuccessful model fit, using the square-root relaxation dispersion profile $T_{1OF} \sim \nu^{1/2}$ (nematic-like) instead of the linear dispersion law $T_{1OF} \sim \nu^1$ (smectic-like).

Computer assisted curve fittings [24] of this model without taking into account cross-effects between the denoted mechanisms, i.e. using

$$1/T_1 = 1/T_{1OF} + 1/T_{1SD} + 1/T_{1DR} + 1/T_{1Rot}, \quad (1)$$

allowed within the experimental errors a quantitative description of the data as illustrated in Figs. 4 and 5 by the full and dotted lines. For comparison, Fig. 6 illustrates an unsuccessful fit based on the square-root law instead of the linear $T_{1OF}(\nu)$ dependence. The details of the individual relaxation rates have been described frequently in the literature [e. g. 4, 10, 16–24] (in particular see Schweikert et al. [24]), and hence are not repeated here explicitly. We only consider the underlying model parameters to discuss the physical meaning of the evaluated quantities, and to this purpose write the four contributions to (1) in the following abbreviated forms:

(i) $$1/T_{1OF} = A\,\nu^{-1} f_{OF}(\nu/\nu_c), \quad (2)$$

where the parameter A is characteristic for the strength of this mechanism, the function f_{OF} describes the transition of the linear frequency dependence to a plateau, and the cut-off frequency ν_c measures the low-frequency limit of the collective mode spectrum, which is responsible for the plateau (Blinc model [20, 21, 24]).

(ii) $$1/T_{1SD} = B\,\tau_{SD} f_{SD}(\nu, \tau_{SD}), \quad (3)$$

where the parameter B is determined by the dipolar coupling between proton spins of neighbouring molecules, i.e. essentially by the effective intermolecular proton-proton separation, the function f_{SD} describes the anisotropy and step width of the self-diffusion process, and τ_{SD} denotes the average translational jump time of the molecules (Abragam-Pfeifer model [16, 19, 24]).

$$\text{(iii)} \quad 1/T_{1DR} = C\,\tau_{DR}\,f_{DR}(\nu, \tau_{DR}), \tag{4}$$

where the parameter C is determined by the dipolar coupling between proton spins in one molecule, i.e. essentially by the effective intramolecular proton-proton separation, the function f_{DR} describes the spectrum of the twofold reorientation process, and τ_{DR} means the rotational jumping time through the self-diffusion along the helix axis (Žumer-Vilfan model [5, 6]).

$$\text{(iv)} \quad 1/T_{1Rot} = D\,\tau_{Rot}\,f_{Rot}(\nu, \tau_{Rot}), \tag{5}$$

where the parameter D reflects the geometry and hindrance potential of the rotating proton pairs, the function f_{Rot} is characteristic for the rotation mechanism, and τ_{Rot} measures the effective time scale of this reorientation (Woessner-Graf model [22–24]).

Further details on (2)–(5) should be looked up in the original literature. The model fits shown in Figs. 4 and 5 led to the eight parameter values A, B, C, D, ν_c, τ_{SD}, τ_{DR}, and τ_{Rot} summarized in Table 2. As expected, the results demonstrate that the OF process is significant for the relaxation dispersion profile at low Larmor frequencies, whereas the SD process dominates in the high frequency regime. At both temperatures, the transition is clearly controlled by the novel DR contribution, which also produces the shallow $T_1\,(1/\vartheta)$ minimum observed in the cholesteric state of the compound (Figure. 3b). The Rot contribution is almost negligible and essentially frequency independent over the whole accessible range.

Unfortunately, this behaviour of the *cholesteric* mesophase could not be directly compared with full T_1 dispersion measurements for the *crystalline* or *glassy* material, because in these cases the poorer quality of the NMR signal (much shorter free induction decays) did not allow reliable field-cycling studies. However, from the different high-field data of Figs. 3a and 3b we conclude that both the OF and the DR process are absent in the two low-temperature phases: On the one hand, the $T_1(\vartheta)$ plots in both diagrams are rather similar at low temperatures, where the crystalline and glassy states overlap ($\vartheta \leqq 37\,^\circ\text{C}$), and thus indicate that the relevant molecular dynamics should also be similar or even identical. On the other hand, if one compares the $T_1(\vartheta)$ plots for $\vartheta \geqq 37\,^\circ\text{C}$, where the crystalline and cholesteric states overlap, the results are strongly different due to the absence of the OF and DR relaxation contributions in the solid sample. Consequently, it is reasonable to suppose that in the glassy sample the two slow molecular reorientations are frozen or at least considerably slowed down to become unobservable by T_1 measurements [10]. Using this concept, the occurrence of the $T_1(\vartheta)$ maximum below both the cholesteric-to-glass and cholesteric-to-solid phase transition can be understood by a change from essentially self-diffusion to rotation controlled relaxation rates.

In accordance with Fig. 3, the temperature dependence of the involved model parameters obtained from the variations between the data of Fig. 4 (50 °C) and Fig. 5 (100 °C) is relatively small, and for some of them even within the experimental error limits. Nevertheless, the observed parameter shifts reveal some aspects which are fully consistent with the formalism of (2)–(5). As seen by Table 2, all the time constants ($1/\nu_c$, τ_{SD}, τ_{DR}, τ_{Rot}) are smaller at 100 °C than at 50 °C, whereas the intensity parameters (A, B, C, D) either slightly increase with higher temperatures or remain approximately constant. This can be explained by the thermal activation of the various reorientations

Table 2. Model parameters obtained by the curve fits of (1)–(5) to the experimental $T_1(\nu)$ data of BET shown in Figs. 4 and 5. The notation is explained in the text and the given references.

Temp.	Order fluctuations		Self-diffusion		Induced rotation		Rotation	
°C	A/s^{-2}	ν_c/kHz	B/s^{-1}	τ_{SD}/ns	C/s^{-1}	τ_{SD}/ns	D/s^{-1}	τ_{Rot}/ns
50	$6.8 \cdot 10^{-8}$	17	$1.4 \cdot 10^{-9}$	10	$4.9 \cdot 10^{-8}$	125	$3.9 \cdot 10^{-8}$	0.23
100	$12 \cdot 10^{-8}$	27	$3.1 \cdot 10^{-9}$	5	$7.2 \cdot 10^{-8}$	70	$3.2 \cdot 10^{-8}$	0.18

and by adequate changes of the molecular or mesophase structure.

(i) The OF relaxation rate is considerably faster for *BET* than for untwisted nematic liquid crystals studied previously [8–10] at comparable temperatures. Though this result is subject to a large error due to the presence of the DR term, it is reasonable as a consequence of the differing viscosity η and the relation $A \sim \eta^{1/2}$ involved in the Blinc model [18, 20, 24]. Between 50 °C and 100 °C, the parameter A increases by a factor of two. Since in our fits the position of the low-frequency $T_1(\nu)$ plateau, which through (2) is determined by $T_1(0) \sim \nu_c/A$, turned out nearly temperature independent, the cut-off frequency ν_c increases by the same factor as A. Both variations can be ascribed basically to a probable change of the coherence length ξ of the OF modes spectrum [24] ($A \sim 1/\xi$, $\nu_c \sim 1/\xi$), which implies that the range of collective motions is reduced at higher temperatures.

(ii) The SD relaxation rate for *BET* is comparable with the data known for nematic mesogens [8–10], where, however, it has often been noticed that the absolute value of the evaluated self-diffusion constant D_S deviates from results of more direct techniques. As a rule, the height and the length of the low-frequency $T_1(\nu)$ plateau are hard to combine with the constraints of (3). In the present case, this point is also a problem, because the jump time τ_{SD} becomes smaller and the intensity parameter B becomes larger with increasing sample temperature. Using the molecular width ($d \sim 5 \cdot 10^{-8}$ cm) as the average closest intermolecular spin approach, we obtain at $\vartheta = 50$ °C from the fitted jump time τ_{SD} the self-diffusion constant $D_S \sim 4.2 \cdot 10^{-8}\,\mathrm{cm^2\,s^{-1}}$; this is in excellent agreement with results of NMR line width studies [7] of cholesteric 4n-octyloxyphenyl-4n′-pentyloxybenzoate, and also with relaxation measurements [4] on the cholesteric phase of cholesteryl-oleylcarbonate. An interesting detail is that the related activation energy (40 kJ/mole), estimated by the comparison of Figs. 4 and 5, has a similar magnitude as known for normal nematic systems, but is much lower than for smectic mesogens [25, 26].

(iii) The DR relaxation rate is a significant contribution, but obviously only in the low-frequency regime: As shown in Table 2, the responsible reorientation time τ_{DR} is longer than τ_{SD} by more than a factor of ten, and this explains why the process has not been observed previously [4]. Whereas the time scales of τ_{SD} and τ_{DR} are strongly different, their temperature dependence as seen by the T_{1SD} and T_{1DR} relaxation dispersion exhibits approximately the same activation energy, i.e. ≈ 40 kJ/mole. This surprising result is confirmed if one further takes into account that the position of the $T_1(\vartheta)$-minimum in Fig. 3b allows an independent more direct determination of the DR jump time at $\vartheta \approx 85$ °C by the minimum condition $2\pi\nu\tau_{SD} = 0.5$ of (4); in view of the different approaches the data at 50, 85, and 100 °C follow, within the error limits, a remarkably satisfying Arrhenius law.

(iv) The Rot relaxation rate is the least reliable contribution of the model fitting since it is only based on minor corrections of the dispersion profile at high Larmor frequencies, where the number of data points is small. Nevertheless, if one estimates the average proton-proton separation $r_{eff} = a$ of rotating spin pairs by (5) in the fast motional limit [16], that means using $D = 3\gamma^4 h^2 \varepsilon/(8\pi^2 a^6)$ and $f_{Rot}(\nu, \tau_{Rot}) = \tau_{Rot}$ with D and τ_{Rot} from Table 2 and a typical anisotropy factor [23] of $\varepsilon = 0.1$, one gets at $\vartheta = 100$ °C the value $a = 1.80 \cdot 10^{-8}$ cm (γ: proton magnetogyric ratio; h: Planck's constant). This compares well with the length $a = 1.78 \cdot 10^{-8}$ cm characteristic for the interproton separation of CH_2 and CH_3 groups. Neglecting the anisotropy of the reorientations ($\varepsilon = 1$) would lead to a much too large effective distance between neighbouring protons ($a = 2.65 \cdot 10^{-8}$ cm), and this finding clearly demonstrates that the analysis is basically correct. However, details on the rotations of individual spin pairs about different axes [22] cannot be evaluated from the available experimental data.

4. Conclusions

Our frequency dependent proton T_1 relaxation dispersion measurements of a liquid crystal with a cholesteric mesophase (*BET*) reveal an additional slow molecular reorientation process, which has not been observed previously in untwisted nematic phases. We assign this process to the rotation of whole molecules induced through the self-diffusion along the helix axis, a relaxation mechanism first suggested, expected and calculated by Andreev [5] and by Vilfan et al. [6]. It is superimposed on the familiar relaxation mechanisms confirmed previously in nematic mesogens [8–10], where T_1 at low Larmor frequencies is usually governed by director order fluctuations and at high frequencies by self-diffusion. The new relaxation mechanism disappears in the glassy state of the com-

pound, though there the compound maintains the cholesteric structure. Most of the basic findings can be understood quantitatively in terms of existing theoretical models on proton spin relaxation in liquid crystals, and thus increase the variety of mesogenic phases with characteristic slow molecular motion effects not seen by standard NMR methods. But one notable detail does not yet agree with the theoretical predictions, namely the occurrence of a linear (i.e. smectic-type) instead of a square-root (i.e. nematic-type) dispersion profile due to order fluctuations. Presently it cannot be decided whether this indicates a two-dimensional restriction of the collective mode spectrum or whether it results from an interference of the two slow reorientations OF, DR) because of their comparable time scales.

Acknowledgements

D. Pusiol and C. Aguilera acknowledge the support of the Alexander von Humboldt Foundation for a research year in Stuttgart and Freiburg, respectively, and also recognize the support of the research program by the Deutsche Forschungsgemeinschaft. All the authors thank the members of the Stuttgart NMR group, in particular Dipl. Phys. K. H. Schweikert, for their extensive experimental and theoretical assistance.

[1] C. R. Dybowski and C. G. Wade, J. Chem. Phys. **55,** 1576 (1971).
[2] R. Y. Dong, M. M. Pintar, and W. F. Forbes, J. Chem. Phys. **55,** 2449 (1971).
[3] C. E. Tarr and M. E. Field, Mol. Cryst. Liq. Cryst. **30,** 143 (1975).
[4] M. Vilfan, R. Blinc, J. Dolinšek, M. Ipavec, G. Lahajnar, and S. Žumer, J. Phys. (Paris) **44,** 1179 (1983).
[5] V. Andreev, Mol. Cryst. Liq. Cryst. **82,** 289 (1982).
[6] S. Žumer, M. Vilfan, and R. Blinc, Proc. 6th European Experimental NMR Conference **1982,** p. 57.
[7] R. Stannarius and H. Schmiedel, J. Magn. Reson. **81,** 339 (1989).
[8] W. Wölfel, F. Noack, and M. Stohrer, Z. Naturforsch. **30 a,** 437 (1975)
[9] F. Noack, M. Notter, and W. Weiß, Liq. Cryst. **3,** 907 (1988).
[10] F. Noack, Prog. Nucl. Magn. Reson. Spectrosc. **18,** 171 (1986).
[11] C. Aguilera, Z. Naturforsch. **42 b,** 113 (1987).
[12] U. Zimmermann, Diplomarbeit, Universität Stuttgart (1989).
[13] S. Hoffmann, W. Brand, and H. Schubert, Z. Chem. **15,** 59 (1975).
[14] S. Hoffmann, W. Brand, and H. Schubert, Z. Chem. **16,** 62 (1979).
[15] M. Stohrer and F. Noack, J. Chem. Phys. **67,** 3729 (1977).
[16] A. Abragam, The Principles of Nuclear Magnetism, Clarendon Press, Oxford 1962.
[17] P. Pincus, Sol. State. Commun. **7,** 415 (1969).
[18] I. Zupančič, V. Žagar, M. Rožmarin, I. Levstik, F. Kogovšek, and R. Blinc, Sol. State Commun. **18,** 1591 (1976).
[19] H. Pfeifer, Ann. Phys. Leipzig **8,** 1 (1961).
[20] R. Blinc, M. Luzar, M. Vilfan, and M. Burgar, J. Chem. Phys. **63,** 3445 (1975).
[21] M. Vilfan, M. Kogoj, and R. Blinc, J. Chem. Phys. **86,** 1055 (1987).
[22] D. E. Woessner, J. Chem. Phys. **37,** 647 (1962).
[23] (a) V. Graf, F. Noack, and M. Stohrer, Z. Naturforsch. **32 a,** 61 (1977); (b) V. Graf, Thesis, Universität Stuttgart, 1980.
[24] K. H. Schweikert and F. Noack, Z. Naturforsch. **44 a,** 597 (1989).
[25] G. J. Krüger, Phys. Rep. **82,** 229 (1982).
[26] F. Noack, Mol. Cryst. Liq. Cryst. **113,** 247 (1984).